HYDROLOGICAL PROCESSES
Hydrol. Process. **18**, 1409–1422 (2004)
Published online in Wiley InterScience (www.interscience.wiley.com). DOI: 10.1002/hyp.1420

The application of depletion curves for parameterization of subgrid variability of snow

Charles H. Luce[1]* and David G. Tarboton[2]

[1] *USDA Forest Service, Rocky Mountain Research Station, Boise, ID 83702, USA*
[2] *Civil and Environmental Engineering, Utah State University, Logan, Utah 84322, USA*

Abstract:

Parameterization of subgrid-scale variability in snow accumulation and melt is important for improvements in distributed snowmelt modelling. We have taken the approach of using depletion curves that relate fractional snow-covered area to element-average snow water equivalent to parameterize the effect of snowpack heterogeneity within a physically based mass and energy balance snowpack model. Comparisons of parameterization outputs with distributed model outputs and observations show performance comparable to the distributed model and reasonable performance relative to observations for time series modelling of snow water equivalent and snow-covered area. Examination of the relationship between the shapes of the depletion curves and parametric distributions shows that the shapes of dimensionless depletion curves depend primarily on the coefficient of variation and to a lesser extent on the shape of the snow distribution function. The methods presented here are a generalization of several previously used methods to estimate depletion curve shapes. Comparison of several years of observed depletion curves from the study basin show that the shapes of the depletion curves change little from year to year. Copyright © 2004 John Wiley & Sons, Ltd.

KEY WORDS distributed snow models; subgrid variability; scale; snow-cover patterns; snow water equivalent

INTRODUCTION

Snow accumulation and melt are spatially variable due to spatial variability of the driving processes and inputs. This variability leads to a nonuniform spatial distribution of snow water equivalent and patchiness in the snow cover during melt. Surface energy fluxes driving snowmelt only melt snow where snow is present, so an important process to consider in the modelling of snowmelt is the evolution in time of snow-covered area. Depletion curves have been developed to characterize the reduction in snow-covered area during the progress of melt.

Depletion curves have historically been used to predict runoff based on temperature-index-based melt estimates (e.g. Anderson, 1973; Martinec, 1980, 1985; Brubaker *et al*., 1996). In such modelling, the amount of melt is multiplied by the snow-covered area to estimate the total input of water to a basin. There is less of a history of using snow-covered area to inform modelled evolution of snow water equivalent in the snowpack (Dunne and Leopold, 1978; Ferguson, 1984; Buttle and McDonnell, 1987; Luce *et al*., 1999). In this sort of modelling, information about the total mass of snow in the area (from direct measurement of the snowpack or estimated from accumulated precipitation) is used, and conservation of mass is considered.

Luce *et al*. (1999) suggested the use of the depletion curve as a parameterization of subgrid variability in a physically based mass and energy balance snowmelt model. In modelling snowmelt over a watershed, the reductionist approach is to apply a 'point' model at many points on a fine grid. This is often impractical, so a subgrid parameterization is necessary to enable modelling with larger model elements. Rather than relating

* Correspondence to: Charles H. Luce, USDA Forest Service, Rocky Mountain Research Station, Boise, ID 83702, USA.
E-mail: cluce@fs.fed.us

Received 9 April 2002
Accepted 15 January 2003

snow-covered area to accumulated melt or degree days, as in earlier depletion curve methods, Luce *et al.* (1999) related snow-covered area to the total mass of snow remaining on the ground, or the area-averaged snow water equivalent. The area-averaged snow water equivalent was normalized by the maximum snow water equivalent experienced by the area during the current season. These modifications addressed two goals: first, they avoided the problem of assigning dates and peak or average depth at onset of melt; second, it avoided the need for a new depletion curve each season. The depletion curve was naturally scaled by maximum snow accumulation in any given year, requiring only a nondimensional functional form of the depletion curve to be specified. Luce *et al.* (1999) derived equations that estimated a dimensionless depletion curve from the distribution function of snow water equivalent at peak snow accumulation. They further demonstrated that a depletion curve estimated from the distribution provided results that were nearly as good as a fully distributed, physically based mass and energy balance model.

The purpose of this paper is to show how dimensionless depletion curves have general application and utility in scaling-up snowmelt models. One of the key points to make in this undertaking is to show that there can be a physical basis for identifying depletion curves, and that they need not be strictly calibration parameters. First, we will show that the subgrid parameterization with a mass and energy balance model preserves the secondary relationship between basin average snow water equivalent and the average snow water equivalent of snow-covered areas. Second, we will show how the shape of the depletion curve relates to the distribution function of the snowpack, leading to the conclusion that the method outlined in Luce *et al.* (1999) is a generalization of previous methods used to estimate depletion curves. Finally, we present a series of observed dimensionless depletion curves from several years in one basin to show how the dimensionless depletion curve is stable over time.

METHODS

Data collection

The data presented in this study were sampled at the Upper Sheep Creek basin of the Reynolds Creek Experimental Watershed. The watershed is in the Owyhee Mountains of southwest Idaho, USA (Figure 1). Upper Sheep Creek is approximately 26 ha in size, but has more heterogeneity in snow accumulation than one might expect at this scale due to drifting caused by strong winds (Figure 2). Most of the basin is covered in sagebrush, but a small portion where there is sufficient moisture supports a small population of dwarf aspen. The site has characteristics typical of semi-arid shrub steppe environments common to North America and Central Asia.

The data used in this study were measurements of snow water equivalent on a grid of 255 stations within Upper Sheep Creek (Figure 2). Such measurements were taken several times each year over the course of

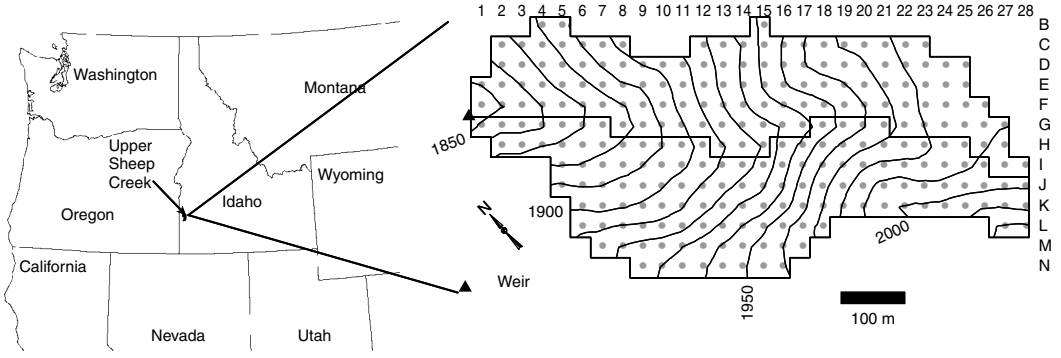

Figure 1. Location map for Upper Sheep Creek and expanded site map showing basin size, orientation (note non-standard north arrow), elevation range (m), and sampling grid on 30·3 m centres

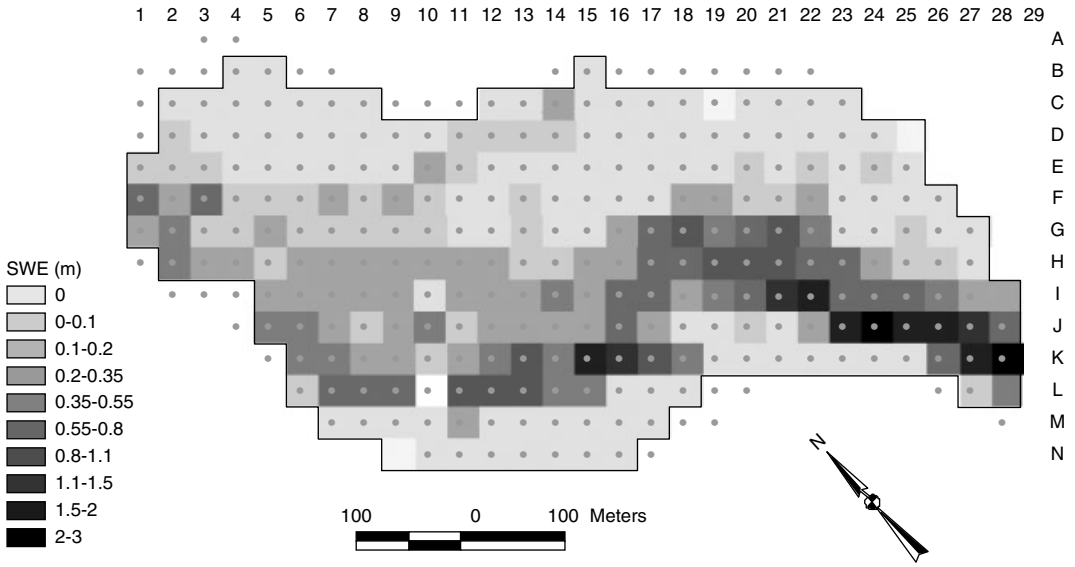

Figure 2. Snow water equivalent measured in Upper Sheep Creek, 3 March 1993. Point L10 was not measured

9 years (Cooley, 1988). In addition, climatic information, such as wind speed, temperature, humidity, solar radiation, and precipitation, were monitored within the watershed. See Hanson (2001; Hanson *et al*., 2001) for details on measurements and quality control.

Summary of model

The model estimates the time evolution of three state variables based on spatially averaged climatic inputs (Figure 3). The three state variables are: (1) W_{sc}, the snow water equivalent of the snow-covered area; (2) U, the snowpack energy content of the snow-covered area; and (3) the fractional snow-covered area A_f. The energy and mass balance of the snow covered area is updated according to

$$\frac{\partial U}{\partial t} = Q_{sn} + Q_{li} - Q_{le} + Q_e + Q_h + Q_g + Q_p - Q_m \tag{1}$$

$$\frac{\partial W_{sc}}{\partial t} = P_r + P_s - M_r - E \tag{2}$$

using the Utah energy balance (UEB) model (Tarboton *et al*., 1995; Tarboton and Luce, 1996), where Q_{sn} is net solar radiation, Q_{li} is incoming longwave radiation, Q_{le} is outgoing longwave radiation, Q_p is advected heat from precipitation, Q_g is ground heat flux, Q_h is the sensible heat flux, Q_e is the latent heat flux, Q_m is heat advected with melt water, P_r is the rate of precipitation as rain, P_s is the rate of precipitation as snow, M_r is the melt rate, and E is the sublimation rate. Snow-surface temperature, a key variable in calculating latent and sensible heat fluxes and outgoing longwave radiation, is calculated from the energy balance at the surface of the snowpack, where there is no storage of energy, and the terms on the right-hand side of Equation (1) (excluding melt) must equal the amount of heat conducted into the snowpack. Conduction is calculated based on a modified force restore equation (Luce and Tarboton, 2001).

Equation (2) is applied only over the fractional snow covered area A_f. The basin average snow water equivalent W_a is given by

$$W_a = W_{sc} A_f \tag{3}$$

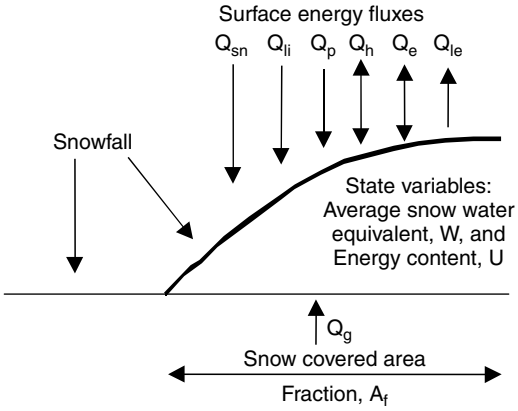

Figure 3. Schematic of lumped snowmelt model. Q_{sn} is net solar radiation; Q_{li} is incoming longwave radiation; Q_{le} is outgoing longwave radiation; Q_p is advected heat from precipitation; Q_g is ground heat flux; Q_h is the sensible heat flux; and Q_e is the latent heat flux

The fractional snow-covered area that parameterizes the subgrid variability and partial coverage of the model element by snow is modelled as

$$A_f = A_{dc}(W_a) \tag{4}$$

where A_{dc} represents the functional relationship between the basin-averaged snow water equivalent and fractional snow-covered area, which is the parameterization we term a 'depletion curve', or more specifically a water equivalent–snow-covered area depletion curve. Below, we discuss other 'depletion curves' in the literature that have related snow-covered area to cumulative snowmelt, or date. We have further suggested that the depletion curve is similar in shape from year to year, changing only in the maximum basin average snow water equivalent W_{amax}. Thus, the particular depletion curve A_{dc} is determined from a dimensionless depletion curve A^*_{dc} and the maximum accumulation to date by

$$A_{dc}(W_a) = A^*_{dc}\left(\frac{W_a}{W_{amax}}\right) \tag{5}$$

Because we never know which day has the maximum until the season is over, we assume that the largest value of W_a experienced from the beginning of the snow season to date is W_{amax}.

In simplified terms, melt is estimated over the snow-covered area, which results in an estimate of the change in mass of the snowpack in the basin. This change in mass is then used as the basis for the estimate of snow-covered area for the next time step. There are some rough approximations in this approach, such as not explicitly accounting for the spatial variation in timing of melt outflow initiation from a snowpack of variable depth. However, Luce *et al*. (1999) demonstrated that the subgrid parameterization performs well in comparison with a fully distributed physically based model (Figure 4). The delay seen in the subgrid parameterization output near the start of the melt season is probably due to this effect, but the error is small because ripening a column of snow requires very little energy compared with the total energy required to melt a column of snow.

A brief description of depletion curves

Figure 5 shows a depletion curve estimated by several methods, as presented by Luce *et al*. (1999). This example serves to illustrate how the depletion curve parameterization is implemented and used. On the left axis is the fractional snow-covered area (ranging from zero to one), and the lower axis is the basin snow water equivalent divided by the seasonal peak snow water equivalent W_{amax}, or the dimensionless basin average snow water equivalent W^* (range zero to one). The basic relationship between snow water equivalent

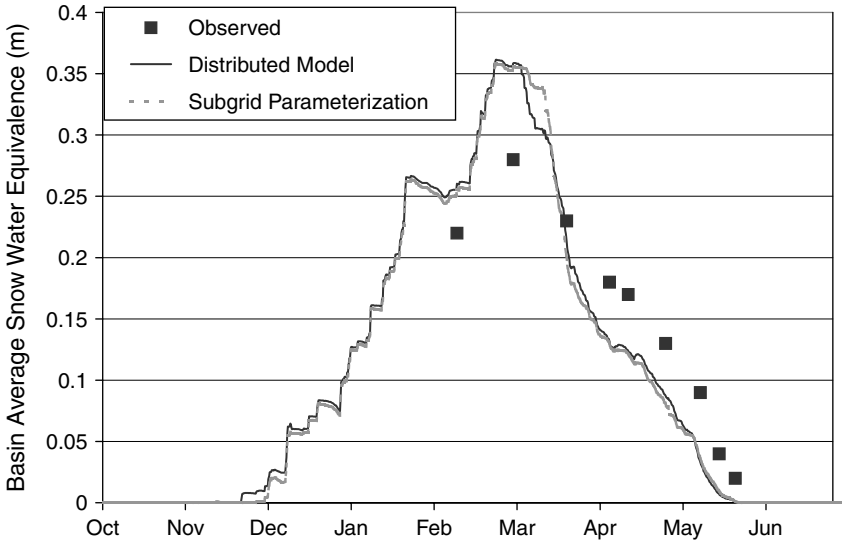

Figure 4. Snow water equivalent over time: observations, distributed model, and lumped model. From Luce *et al.* (1999)

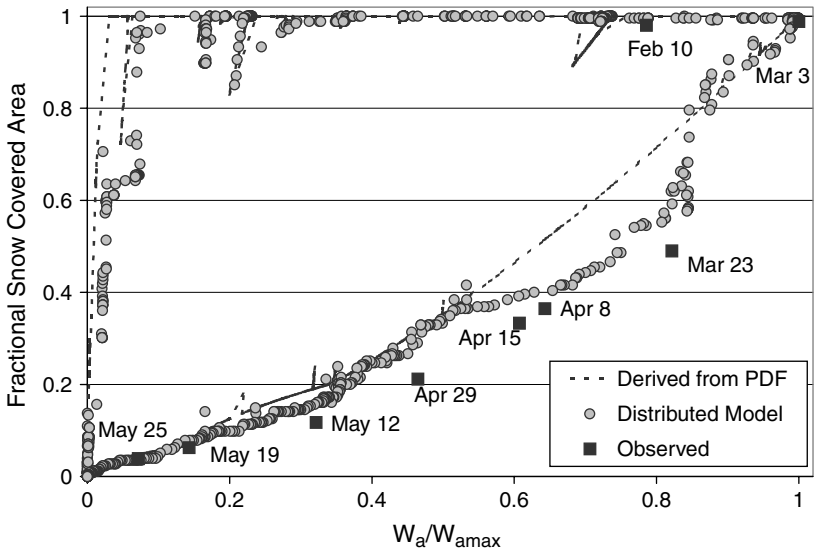

Figure 5. Depletion curve for Upper Sheep Creek derived by three methods: (1) from p.d.f. of snow water equivalent on 3 March 1993; (2) from distributed model outputs; (3) from observations. Note hysteresis in relationship as snow covers entire area with only slight accumulation in early season (on left), whereas melt uncovers areas gradually. From Luce *et al.* (1999)

in a basin and the fractional cover is hysteretic in nature. During accumulation, A_f increases to full cover quickly with initial snowfall, and stays at full cover until melt begins, at which point there is a gradual reduction in fractional area as the basin average snow water equivalent is reduced by melt. In Figure 5, we see accumulation without change in cover between 10 February and 3 March, and a decline in both A_f and W^* as the melt season progresses.

There are, of course, deviations from this simple plan, such as a melt event during what is generally an accumulation phase, or an accumulation event during what is otherwise generally a melt phase. Early melt

events are not distinguished from the main seasonal melt in how they are handled. Each melt event is assumed to be the major melt event and follow the main depletion curve. If later events create accumulations such that the W_{amax} of the earlier melt event is exceeded, then it will come to be shown as an 'early' event. Late accumulation events require the model to track 'new' snow relative to old snow and temporary rescaling of the depletion curve to handle the melt of the new snow. The full details of how such excursions are handled is discussed by Luce *et al.* (1999).

The original depletion curve developed by Anderson (1973) relates snow-covered area to cumulative snowmelt. The 'depletion curve' name has also been used to describe functions that relate snow-covered area to date, cumulative degree days, or melt (e.g. Martinec, 1985; Buttle and McDonnell, 1987; Brubaker *et al.*, 1996), and in our earlier work we also used this name for the function that related snow-covered area to basin or area average snow water equivalent. One of the benefits of using a dimensionless depletion curve that relates reduction of snow-covered area to reductions in W_a/W_{amax}, rather than to date, to cumulative degree days or to cumulative melt, is that it accounts naturally for the variability in year-to-year snow amounts, so that a single depletion curve can be used for different years. It also enables the reduction of snow-covered area be determined naturally from the onset of melt modelled using physical processes, rather than using parameters to determine the beginning of the melt season.

Estimating depletion curves

The dimensionless depletion curve, $A^*_{dc}(W^*)$, may be estimated from the probability density function (p.d.f.) of snow water equivalent sampled spatially (Luce *et al.*, 1999). Implicit in that derivation are the assumptions that spatial variability is created primarily by differential accumulation and that melt is uniform. We know that melt is, in reality, nonuniform, and Luce (2000) demonstrated that if variation in accumulation and variation in melt rate are inversely correlated, as in the case of Upper Sheep Creek, then the effect of including variation in melt is equivalent to having a greater variance in accumulation under uniform melt. However, Luce *et al.* (1998) noted that most of the spatial variability in Upper Sheep Creek was due to variations in accumulation, not variations in melt, and for simplicity of presentation of the concepts in this paper we discuss only the case of uniform melt.

If we apply a uniform melt to a distribution of snow water equivalent depths, then the increase in fractional area will be the proportion of depths that are less than the melt. The concept was presented for a Gaussian distribution by Dunne and Leopold (1978) but generalized by Luce *et al.*, (1999)

$$A_f(M) = 1 - F_g(M) \tag{6}$$

where M is the accumulated depth of snow water equivalent melted since peak accumulation and F_g is the cumulative distribution of snow water equivalent at peak accumulation. Recognizing that the basin average snow water equivalent can be represented as the sum of a series of thin layers of equal snow water equivalent, dw, one can see (Figure 6) that the basin average water equivalent as a function of the accumulated melt can be obtained from

$$W_a(M) = \int_M^\infty A_f(w)\ \mathrm{d}w \tag{7}$$

The snow water equivalent–snow-covered area depletion curve may then be found from

$$A^*_{dc}\left(\frac{W_a(M)}{W_{amax}}\right) = A_f(M) \tag{8}$$

evaluated at many values of M, noting that

$$W_{amax} = W_a(M = 0) \tag{9}$$

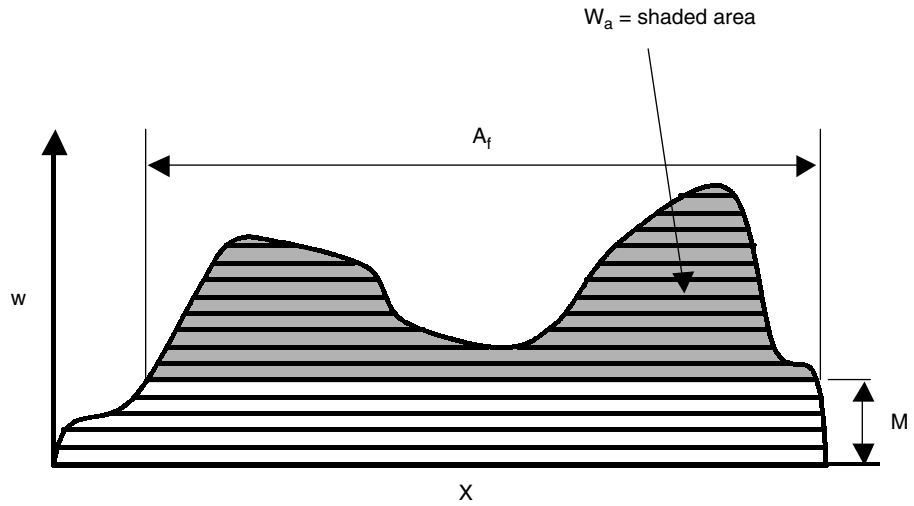

Figure 6. Schematic of snowpack showing how W_a can be estimated as an integral of $A_f(w)$

Practically speaking, Equations 6–9 can be evaluated numerically for a sample of snow water equivalent values. For a series of values M_i, ranging from zero to the maximum observed snow water equivalent ($M_1 = 0$ and M_n is the maximum snow water equivalent, where n is the total number of values in the series), the number of samples with snow water equivalent greater than the M_i divided by the total number of samples is an estimate of $A_f(M_i)$. $W_a(M_i)$ is the sum of $A_f(M_j)$ for all $M_j > M_i$, or more formally:

$$W_a(M_i) = \sum_{j=i}^{n} A_f(M_j) \tag{10}$$

Dividing each value of $W_a(M_i)$ by W_{amax} gives $W^*(M_i)$. Plotting $A_f(M_i)$ against $W^*(M_i)$ provides a descriptive shape that can be fitted with a functional curve for simple application in a snowmelt model.

In the absence of observations at the peak snow water equivalent, simulation may be useful to estimate the distribution of snow water equivalent in an area of interest. Empirical approaches (e.g. Elder *et al.*, 1998; Winstral *et al.*, 1999) can be used to extrapolate data from one area to another similar area. Physically based approaches (e.g. Liston and Sturm, 1998) would seemingly reduce risks associated with extrapolation. Prasad *et al.* (2000) noted that the drifting model of Liston and Sturm (1998) did not match exact locations of drifts on the landscape, but that the modelled p.d.f. of snow water equivalent over an area was close to the observed p.d.f. Sequential imagery of snow-covered area (e.g. Rosenthal and Dozier, 1996) combined with modelled melt estimates could also be used to estimate depletion curves.

Analyses

To assess the performance of the model further, with respect to its modelling of snow-covered area and snow water equivalent, we plotted snow-covered area as a function of time and the relationship between W_{sc} and W_a for the season modelled in Figure 4 (water year 1993). To do this, a distributed model was also used to represent the basin. The distributed model uses the same energy balance as the lumped model described above, but it was run on 255 model elements within the basin, each comprising a square cell of 30·3 m on a side. We assumed no variability in snow accumulation or melt within these elements; so, effectively, each had a depletion curve with $A_f = 1{\cdot}0$ for all values of W^*, except that $A_f = 0$ when $W^* = 0$. Temperature was adjusted for elevation within the basin, and solar radiation was adjusted for terrain attributes.

To show that the parameterization is flexible enough to represent a range of possibilities, we performed a sensitivity analysis of the shape of the depletion curve on the choice of distribution function and parameters to the function. Distributions examined included a uniform distribution (as applied by Ferguson (1984)), normal distribution (Dunne and Leopold, 1978; Buttle and McDonnell, 1987), lognormal distribution, and gamma distribution.

To measure the variation between depletion curves in different years, we summarized 9 years of surveys with the basin average snow water equivalent for each survey and the snow-covered area for each survey. The basin average snow water equivalent from each survey was divided by the maximum basin average snow water equivalent measured in each year.

RESULTS AND DISCUSSION

Modelling additional variables and relationships

One argument for the generality of this approach to depletion curves is that there is a physical basis for them. The shape of the depletion curve can be estimated directly from physically observable information on the distribution of snow water equivalent in a basin, and the accumulation and melt can be predicted from physically observable climatic variables. The testing presented so far (Luce *et al*., 1999) has shown that the time pattern of snow water equivalent is reasonably well represented (Figure 4). Because snow-covered area is another useful output from the subgrid parameterization, it is useful to look at the model performance for snow-covered area and derivative relationships. Figure 7 shows the time evolution of the snow-covered area for the time period depicted in Figure 4. In Figure 7, we see that, for this period, the modelling of snow-covered area was similar in quality to the modelling of snow water equivalent.

Figure 8 shows the relationship between the average snow water equivalent of snow-covered areas and the basin average snow water equivalent during the periods modelled in Figures 4, 5, and 7. Note that there is a hysteresis, with time going counter-clockwise around the loop, so that the roughly linear portion along the bottom of the graph is the part representing accumulation and is roughly on the 1 : 1 line. The reversal in trend of W_{sc} in the upper left corner of the graph is an important feature. Depletion curves that do not approach the origin correctly will result in W_{sc} values going towards a constant or towards infinity.

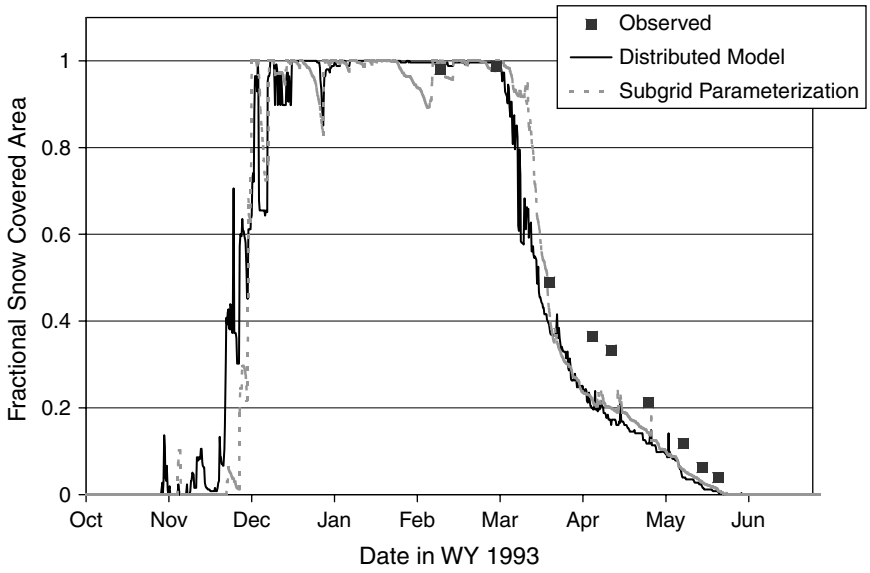

Figure 7. Snow-covered area over time: observations, distributed model, and subgrid parameterization

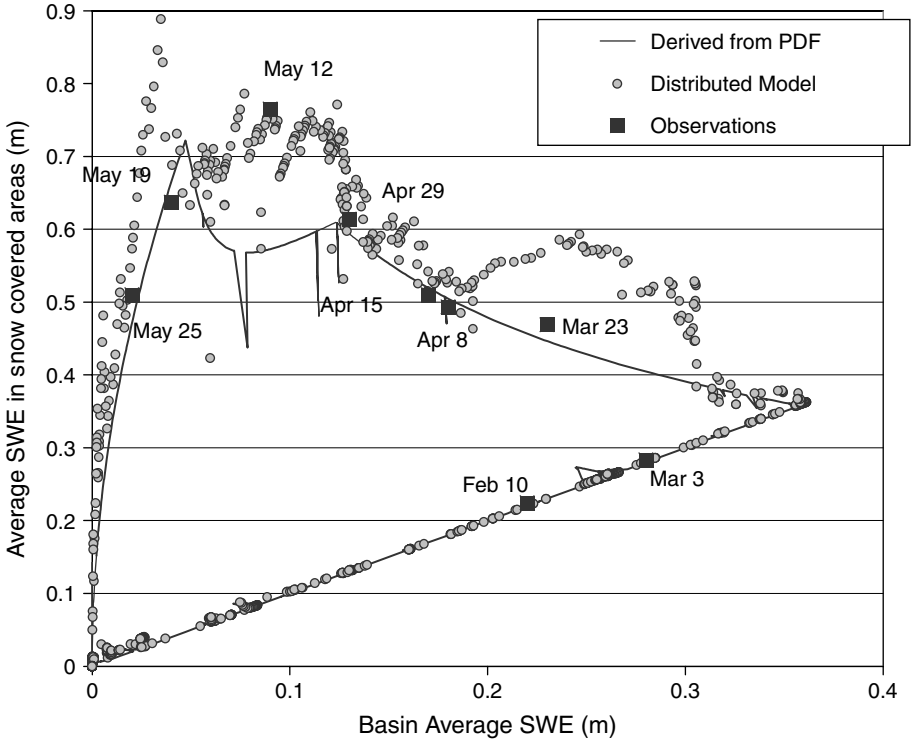

Figure 8. Average SWE of snow-covered areas (W_{sc}) versus average snow water equivalent in basin (W_a) at Upper Sheep Creek in the winter of 1993

The relationship between W_{sc} and W_a modelled by the subgrid parameterization compares reasonably well with observations, as well as with the relationship modelled by the distributed model. For some situations it is difficult to detect model errors visually in the amount of snow water equivalent in snow-covered areas W_{sc} from Figures 4, 5, and 7. For example, at very small values of W_a and A_f, it may not be easy to distinguish the trends if A_f is dropping to small values faster than W_a (a relationship set by the depletion curve). The model may actually predict increases in W_{sc} during periods when W_{sc} and A_f are both falling. The plot of W_{sc} versus W_a is, therefore, a useful additional test or diagnostic when identifying a depletion curve.

Examination of depletion curve graphs (plotted as A_f versus W_a) reveal that their shape holds useful insights related to the melt process. The slope of the curve at any point describes how the snowpack is melting. The slope of the curve is dA_f/dW_a, which estimates the decrement in area for any decrement in snow water equivalent. Recall from Equation (3) that the basin average snow water equivalent W_a is the fractional snow-covered area A_f times the average snow water equivalent of the snow-covered area, defined as W_{sc} above. Lines radiating from the origin of a depletion curve then would be lines of constant W_{sc} with a line of $W_{sc} = 0$ vertical from the origin and $W_{sc} \to \infty$ as it approaches the horizontal axis. From any point along the depletion curve, there is a line from the point to the origin along which W_{sc} is constant. If the slope of the depletion curve is the same as this slope, then incremental melt yields no change in the average snow water equivalance of snow-covered areas. If the slope of the depletion curve is steeper than that line, then the area is decreasing faster than the basin average water equivalent given the current areal coverage, and W_{sc} increases. If the curve is flatter, then W_{sc} is decreasing.

This information is useful in developing a quantitative intuition about the shape of depletion curves. The snowpack described by the depletion curve in Figure 5 had a great deal of variability, with large areas of shallow snow and a smaller area with very deep snow. A uniform snowpack, uniformly melted, results in

decreases of W_a and W_{sc} with no change in A_f, so would be plotted as a straight line across the top of Figure 5 only dropping to zero area as $W_a \rightarrow 0$.

This information also shows us that, as the origin is approached, the shape of the depletion curve must be concave downward with a vertical slope right at the origin. As snow finally melts away, all three W_a, W_{sc}, and A_f must go to zero simultaneously. A concave upwards depletion curve would have W_{sc} increase as the origin is approached. Any function asymptotic to the horizontal axis will predict a depth of the snow-covered area approaching infinity as the area goes to zero to yield $W_a = 0$. A function arriving along a straight line (not the vertical axis) would imply a finite depth with no area. A function arriving at the vertical axis implies a snow-covered area with no depth, another undefined event. A curve asymptotic to the vertical axis near the origin would have a slope flatter than the direct line to the origin, implying that, at the end, a decrease in W_{sc} is needed to melt a snowpack away. Though there is a temptation to fit a curve such as that seen in Figure 5 with a simple function like $A_f = (W_a/W_{amax})^2$, it can be seen from this discussion that this would be a mistake. Similar caution must be taken with derivations from parametric distributions that allow for a small probability of very large depths. We used a piecewise function to fit the shape of the depletion curve for Figure 5, with a square-root function for the final piece near the origin (Luce *et al*., 1999). Any function of the form $A = cW^b$ with $b < 1$ is acceptable, because $dA/dW = bcW^{b-1}$, which for $b < 1$ tends to infinity as $W \rightarrow 0$.

Sensitivity to parametric distributions

In considering the parameterization of variability, p.d.f. are a common and direct approach. A key idea used in the Luce *et al*. (1999) work was the connection between depletion curves and a density or distribution function parameterization of variability. This idea has been explored previously with normal distributions (Dunne and Leopold, 1978), but it had not been generalized to other distributions or nonparametric (data-based) distributions. Further insight about the subgrid parameterization can be gained from examination of the sensitivity of depletion curves to the choice of parametric distribution and to the choice of parameters for those distributions. Figure 9 shows depletion curves developed from four different parametric distributions considering the distribution parameters. In each case, the depletion curve varied with the distribution parameters only in so far as those parameters changed the coefficient of variation (CV). This is due to the expression of the depletion curve in terms of a normalized snow water equivalent $W^* = W_a/W_{amax}$. For a distribution with a fixed functional form, W_{amax} is proportional to the mean $\overline{W}$ used in the evaluation of the CV. Setting the minimum value as a ratio of the maximum in the uniform distribution essentially parameterizes that distribution on the CV; and with the physically imposed constraint of a zero minimum, the CV can range from a maximum of 0·577 to a minimum of zero. It is interesting to note in Figure 9 how similar the depletion curves are for different distribution functional forms but the same CV, which suggests that the CV is more important than the specific distribution functional form in parameterizing snow-covered area depletion, and further suggests potential for estimating depletion curves for a range of environments. For example, it is generally recognized that windswept areas have greater variability relative to average accumulations than do forested areas. Likewise, larger model elements would likely have greater CVs than small ones for a range of element sizes.

Ferguson (1984) chose a depletion curve based on a uniform distribution between zero and a maximum (his model c) as the best model for his data. That model is fully described in the lower dimensionless depletion curve of Figure 9a. Similarly, the model of Dunne and Leopold (1978), also used by Buttle and McDonnell (1987), was based on a normal distribution. The modifications proposed by Buttle and McDonnell (1987) to account for nonuniform melt would result in a skewed distribution (e.g. something close to lognormal or gamma). The skew results from an assumption that melt varies inversely with accumulated depth. Each of the cases provided thus far in the literature, therefore, is a specific instance of the dimensionless depletion curves shown here. The fact that these earlier papers showed some benefit for modelling in other environments suggests that the more general model will be useful in environments other than Upper Sheep Creek. Deviations

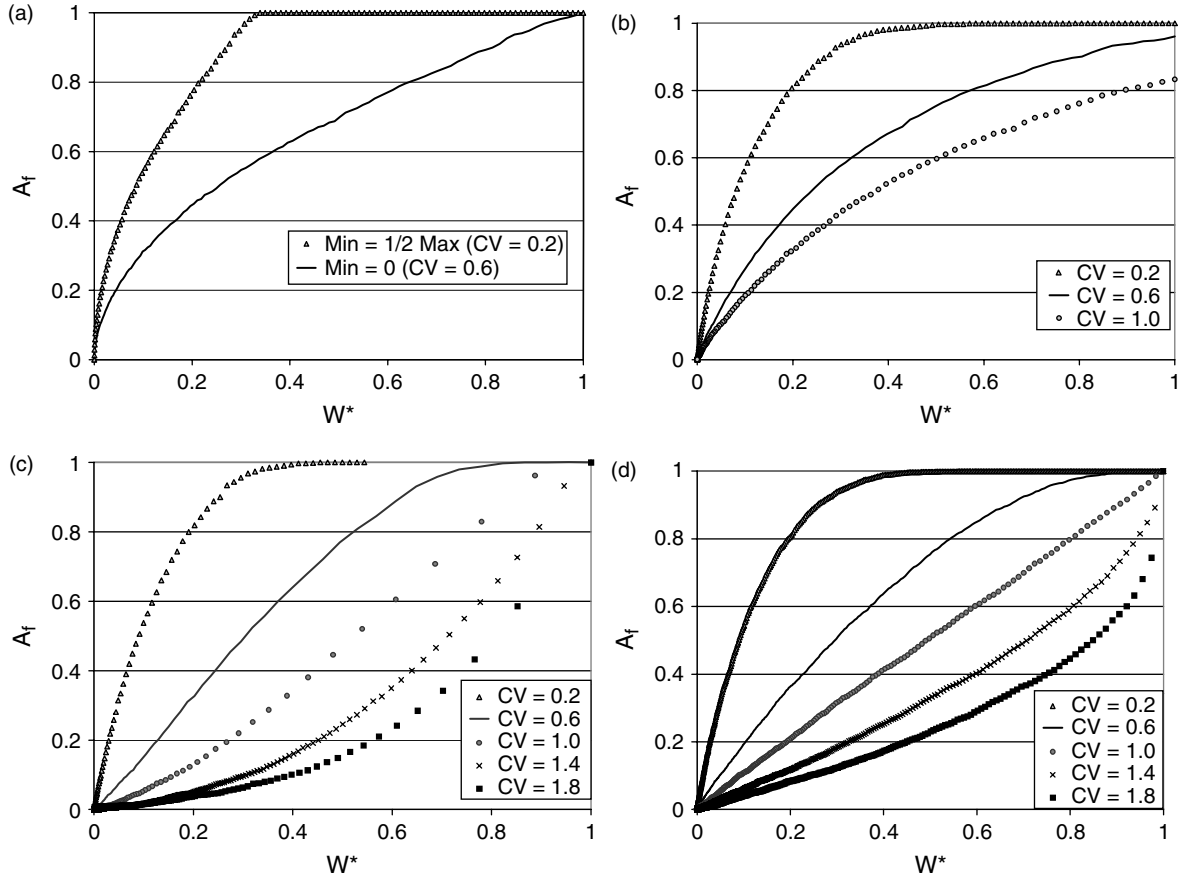

Figure 9. Sensitivity of dimensionless depletion curve shape to choice of distribution and parameters of distributions for (a) uniform distribution, (b) normal distribution, (c) lognormal distribution, and (d) gamma distribution. For the normal distribution, values less than zero were taken as zero

from observations in the earlier models may, in part, be related to poor estimates of the snow distribution, a position supported by the relative performance of the normal distribution for the three cases presented by Buttle and McDonnell (1987: figure 3). Ferguson (1984) and Buttle and McDonnell (1987) made their choices, in part, for computational convenience. Given that the dimensionless depletion curve can be derived from observed or assumed distributions, it becomes more practical to consider more realistic distributions for particular locations.

Multiple years

Snow accumulation varies between years, theoretically requiring a different time-based or melt-based depletion curve for each year dependent on the peak accumulation of the year or melt rate. However, if the relative spatial pattern is consistent, as might be suggested by invariant topography and physically forced wind directions (Kirnbauer and Blöschl, 1994; Sturm *et al*., 1995), then it may be possible to use a dimensionless depletion curve such as that proposed by Luce *et al*. (1999) as a standard from year to year. Indeed, when the dimensionless depletion curves for several years are plotted together, there is a substantial degree of consistency for years, with maximum basin average snow accumulations ranging from 0·10 m in 1991 to 0·28 m in 1993 (Figure 10). It is clear from Figure 9, and some consideration of variations in natural systems, that the set of possibilities for depletion curves occupies much of the space in the unitary square

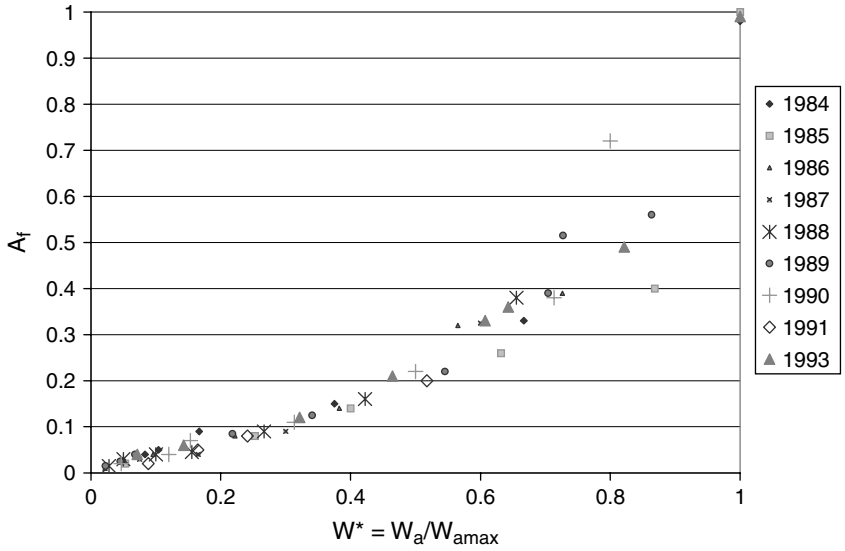

Figure 10. Depletion curves from several years of data at Upper Sheep Creek (data provided by K. Cooley)

defined by $A_f(0:1)$ and $W^*(0:1)$. The nine curves defined by the observations in Figure 10 occupy a small portion of that variation.

In some regard, this is not too surprising for a windswept environment like Upper Sheep Creek. Much wind redistribution happens during snow accumulation, because this is when snow is easily suspended in the air. The surface winds during the largest accumulations tend to be from the southwest, because of where fronts form during cyclonic passage. This is a behaviour fixed by fluid mechanics and the rotation of the Earth. In addition, wind speeds in this location are often high enough that deposition in the lee of ridges and bushes is caused by separation of flow, as opposed to something subtle like variations in wind speed. So, the snow deposits in the same places the same way every year, and all that varies is the amount of snow, which would affect the size of the deposits more than the shape (so as not to over generalize, there would be some effect on the shape, just less so than the amount). In such a case we would expect the standard deviation to track with the mean, yielding small changes in the CV from year to year. In forests that have deep snowpacks, variations would likewise be expected to be minor.

Note that similarity of dimensionless depletion curves from year to year is not a necessary property for their use; however, it is important for any use in a predictive role. It is likely that there are environments or scales for which dimensionless depletion curves change from year to year, and it would be important to understand the causes for the changes.

CONCLUSIONS

Three primary conclusions can be stated: (1) the subgrid parameterization of a mass and energy balance snowmelt model preserves the secondary relationship between snow-covered area and snow water equivalent as a function of time, in addition to the direct relationship between A_f and snow water equivalent; (2) dimensionless depletion curves depend primarily on the CV and to a lesser extent on the shape of the snow distribution function, and are a generalization of previously presented methods for depletion curve estimation; and (3) depletion curves observed over the course of 9 years in the study basin show little variability.

The fact that the model gives reasonable estimates of the time evolution of snow water equivalent and snow-covered area and derivative relationships between area and snow water equivalent supports its applicability

beyond the study basin. There are no adjustable calibration factors available for the model. The distribution of snow at peak accumulation was observed and used to estimate the shape of the depletion curve, which was then used with a physically based snowmelt model to estimate snow accumulation and melt.

Luce *et al*. (1999) showed how to estimate the shape of the depletion curve from the distribution function of snow water equivalent at peak accumulation. In this paper, we show the sensitivity of the shape of the depletion curve to the shape of parametric distribution functions (e.g. gamma or normal). Previously used depletion curves were derived from specific assumed distributions, and such validation of the approach as exists in those in other environments would apply. There is some suggestion that a better estimate of the distribution might yield a better fit to the observations in those studies. There is also a clear utility in adaptation of the dimensionless depletion curve approach to existing temperature-index-type models. If observations in several environments give a better idea as to how distributions of snow water equivalent change with location and vegetation, then the observations can be used directly to inform the shape of depletion curves. If they can be defined better based on physical attributes of the areas they represent, then it is less likely they will require site-specific calibration.

The fact that 9 years of dimensionless depletion curves measured in the study basin show a high degree of similarity (compared with the range of alternatives) suggests that the dimensionless depletion curve approach may be practical for forecasting in areas where the shape can be determined from observation. There is also a potential utility in being able to use estimates of snow-covered area from remote sensing (e.g. Rosenthal and Dozier, 1996) to estimate the proportion of the maximum snow water equivalent still remaining within an area. These uses are only reasonable if there is consistency in the depletion curve from year to year.

One area of research that would considerably increase the utility of depletion curves is for more observations from many environments of the distribution of snow water equivalent values. Although there are general hints based on physical reasoning of how such distributions might look, observations would provide a stronger basis for depletion curve estimates. Such information would probably be helpful in identifying the types of situation that would likely create variations in the shape of depletion curves from year to year. Knowledge of such areas and how the depletion curve is affected by interannual variations in weather are essential to better modelling of larger areas.

ACKNOWLEDGEMENTS

This research was supported by the NASA Land Surface Hydrology Program, grant number NAG 5-7597. The views and conclusions expressed are those of the authors and should not be interpreted as necessarily representing official policies, either expressed or implied, of the US Government. We would like to thank Keith Cooley for the use of data collected at Upper Sheep Creek between 1988 and 1996, for his foresight in collecting such an interesting data set, and for discussions about depletion curves. Our thanks also go to Mark Seyfried, Clayton Hanson, and others at the Agricultural Research Service Northwest Watershed Research Center for providing weather and topographic data for these analyses. Rajiv Prasad's assistance in construction of the distributed model used in these analyses is also appreciated. The manuscript has benefited from review by Kelly Elder and three anonymous reviewers.

REFERENCES

Anderson EA. 1973. *National Weather Service river forecast system–snow accumulation and ablation model*. NOAA Technical Memorandum NWS HYDRO-17, US Department of Commerce, Silver Spring, MD.

Brubaker K, Rango A, Kustas W. 1996. Incorporating radiation inputs into the snowmelt runoff model. *Hydrological Processes* **10**: 1329–1343.

Buttle JM, McDonnell JJ. 1987. Modelling the areal depletion of snowcover in a forested catchment. *Journal of Hydrology* **90**: 43–60.

Cooley KR. 1988. Snowpack variability on western rangelands. In *Proceedings of the 56th Western Snow Conference*, 18–20 April, Kalispell, Montana; 1–12.

Dunne T, Leopold LB. 1978. *Water in environmental planning*. W. H. Freeman and Co.: San Francisco.

Elder K, Rosenthal W, Davis R. 1998. Estimating the spatial distribution of snow water equivalence in a montane watershed. *Hydrological Processes* **12**: 1793–1808.
Ferguson RJ. 1984. Magnitude and modeling of snowmelt runoff in the Cairngorm mountains, Scotland. *Hydrological Sciences Journal* **29**: 49–62.
Hanson CL. 2001. Long-term precipitation database, Reynolds Creek Experimental Watershed, Idaho, United States. *Water Resources Research* **37**: 2831–2834.
Hanson CL, Marks D, Van Vactor SS. 2001. Long-term climate database, Reynolds Creek Experimental Watershed, Idaho, United States. *Water Resources Research* **37**: 2839–2842.
Kirnbauer R, Blöschl G. 1994. How similar are snow cover patterns from year to year? *Deutsche Gewässerkundliche. Mitteilungen* **37**: 113–121.
Liston GE, Sturm M. 1998. A snow-transport model for complex terrain. *Journal of Glaciology* **44**: 498–516.
Luce C. 2000. *Scale influences on the representation of snowpack processes*. Phd dissertation, Utah State University, Logan, UT.
Luce CH, Tarboton DG. 2001. A modified force-restore approach to modeling snow-surface heat fluxes. In *Proceedings of the 69th Annual Meeting of the Western Snow Conference*, 13–17 April, Sun Valley, ID; 103–114.
Luce CH, Tarboton DG, Cooley KR. 1998. The influence of the spatial distribution of snow on basin-averaged snowmelt. *Hydrological Processes* **12**: 1671–1683.
Luce CH, Tarboton DG, Cooley KR. 1999. Subgrid parameterization of snow distribution for an energy and mass balance snow cover model. *Hydrological Processes* **13**: 1921–1933.
Martinec J. 1980. Snowmelt-runoff forescasts based on automatic temperature measurements. In *Hydrological Forecasting*. IAHS Publication No. 129. IAHS Press: Wallingford; 239–246.
Martinec J. 1985. Snowmelt runoff models for operational forecasts. *Nordic Hydrology* **16**: 129–136.
Prasad R, Tarboton DG, Liston GE, Luce CH, Seyfried MS. 2000. Testing a blowing snow model against distributed snow measurements at Upper Sheep Creek. *Water Resoures Research* **37**: 1341–1356.
Rosenthal W, Dozier J. 1996. Automated mapping of montane snow cover at subpixel resolution from the Landsat thematic mapper. *Water Resoures Research* **32**: 115–130.
Sturm M, Holmgren J, Liston GE. 1995. A seasonal snow cover classification system for local to global applications. *Journal of Climate* **8**: 1261–1283.
Tarboton DG, Luce CH. 1996. Utah energy balance snow accumulation and melt model (UEB), computer model technical description and users guide. Utah Water Research Laboratory and USDA forest service intermountain research station. (http://www.engineering.usu.edu/dtarb/) Accessed 10 January 2004.
Tarboton DG, Chowdhury TG, Jackson TH. 1995. A spatially distributed energy balance snowmelt model. In *Biogeochemistry of Seasonally Snow-Covered Catchments*, Tonnessen KA, Williams MW, Tranter M (eds). IAHS Publication No. 228. IAHS Press: Wallingford; 141–155.
Winstral A, Elder K, Davis R. 1999. Implementation of digital terrain analysis to capture the effects of wind redistribution in spatial snow modeling. In *Proceedings of the 67th Western Snow Conference*, South Lake Tahoe, CA; 81–93.

